3-D assessment of gaze-induced eye shape deformations and downgaze-induced vitreous chamber volume increase in highly myopic eyes with staphyloma

Quan V Hoang ,[1,2] Stanley Chang,[2] Daryle Jason Go Yu ,[1] Lawrence A Yannuzzi,[3] K Bailey Freund,[3] Jack Grinband[4]

[1]Singapore Eye Research Institute, Singapore National Eye Centre, Duke National University of Singapore, Singapore
[2]Ophthalmology, Columbia University College of Physicians and Surgeons, New York City, New York, USA
[3]Vitreous Retina Macula Consultants of New York, New York, New York, USA
[4]Radiology, Columbia University College of Physicians and Surgeons, New York City, New York, USA

Correspondence to
Quan V Hoang, Singapore Eye Research Institute, Singapore National Eye Centre, Duke-NUS, 20 College Rd, Singapore, Singapore;
donny.hoang@singhealth.com.sg

Received 17 February 2020
Revised 8 July 2020
Accepted 20 July 2020
Published Online First 23 August 2020

To cite: Hoang QV, Chang S, Yu DJG, *et al*. *Br J Ophthalmol* 2021;**105**:1149–1154.

ABSTRACT

Purpose To determine if the stress of normal eye movements results in gaze-induced globe deformations, vitreous chamber axial length and vitreous chamber axial volume (VCAV) change in highly myopic eyes.

Methods A prospective imaging study was performed on 82 eyes of 43 patients with high myopia (>27 mm of axial length) with a clinical diagnosis of staphyloma. Three-dimensional MRI scans were acquired while subjects gazed in five directions (primary, nasal, temporal, superior and inferior). Surface renderings were generated, and a processing pipeline was created to automate alignment of the eye and to measure VCAV within 5.5 mm of the visual axis for each eye in every gaze. The degree of gaze-induced globe deformation was determined by calculating the Dice coefficient to assess the degree of overlap of the sclera at each eccentric gaze with that found in primary gaze. Each eccentric gaze VCAV was compared to VCAV in primary gaze using a fixed-effects regression allowing for subject-specific and eye-specific effects.

Results The Dice coefficient showed significant gaze-induced eye shape changes in all gazes (all p<0.0001). There were no statistically significant gaze-induced VCAV changes when comparing primary gaze to nasal, temporal or upgaze. However, when changing from primary to downgaze, VCAV was increased by +4.79 mm^3 (p=0.002, 95% CI 1.71 to 7.86).

Conclusion Significant gaze-induced globe deformation was noted in all gazes, but a reversible, instantaneous VCAV increase occurred only in downgaze, which is consistent with studies supporting the association of environmental factors such as near work with myopia development and progression.

Myopia, or near-sightedness, affects up to 80% of the school-age population in parts of Asia[1] and represents a leading cause of blindness.[2] With a rising global prevalence,[3 4] by 2050, it is estimated that 4.8 billion people will have myopia worldwide, of which almost a billion will have high myopia.[5] It is widely accepted that in addition to an epidemic of myopia in developed countries in East and Southeast Asia, there is also an epidemic of high myopia.[6] A vast majority of myopia cases are characterised by excessive axial elongation of the eye over time.[7] 'High myopia', which is defined as greater than 26 mm of ocular axial length or −5.0 D of near-sightedness,[5] represents 20%–30% of the myopic population. High myopia is often complicated by vision-threatening complications such as retinal detachment and posterior staphyloma.[8] The sclera of these extremely elongated eyes show marked thinning,[9 10] and in some eyes, scleral thinning occurs to the extent that local outpouchings (staphylomas) form.[11] Recent reports note that a greater grade of staphyloma is associated with further eye elongation and more severe and progressive myopic maculopathy.[4 11–13]

Both genetic and environmental factors are thought to contribute to axial elongation in myopia.[2] Several reports have noted significant associations between near work and the development and progression of myopia in childhood[14–16] as well as in adults with near work-intensive occupations.[17] Ocular changes that accompany near work include accommodation, convergence and downgaze. Accommodation (involving the ciliary muscle) and convergence (involving extraocular muscles) have been suggested to be involved in myopia progression and result in transient axial elongation during near work.[18 19] Using optical low-coherence reflectometry to measure axial length, Ghosh *et al*[20] found small changes in axial length associated with shifts in gaze, suggesting that extraocular muscle tension on the globe can result in eye length changes for certain angles of gaze. Additionally, MRI has been employed to better examine the three-dimensional shape of staphyloma and scleral contour in highly myopic human eyes.[21–23] Given that near work typically involves accommodation, convergence and downward gaze, we investigated the influence of gaze position on (1) global eye shape, (2) vitreous chamber axial length and (3) vitreous chamber axial volume (VCAV) by using gaze-controlled MRI in the primary and four cardinal positions of secondary gaze.

METHODS

This study complied with the Health Insurance Portability and Accountability Act of 1996 and adhered to the tenets of the Declaration of Helsinki. Institutional Review Board/ethics committee approval was obtained from Columbia University. All patients signed a written consent form before initiation of the study-specific

procedures. Subjects (n=43; 28 females) aged 30–83 years (mean=60 years, SD=14 years) with a clinical diagnosis of high myopia (axial lengths >27 mm on partial coherence interferometry) and staphyloma were enrolled and underwent a complete clinical examination including axial length measurements on IOLMaster (Carl Zeiss Meditec, Dublin, CA, USA), dilated fundus examination, B-scan ultrasonography (Quantel Aviso, Rockwall, TX) and swept-source optical coherence tomography (SS-OCT, DRI October-1, Atlantis, Topcon, Oakland, NJ, USA). B-scan and SS-OCT images for all subjects were screened to detect the presence of staphyloma (defined as an abrupt change in scleral curvature), which were subsequently verified in all cases on MRI. Of the 43 subjects, 1 had unilateral high myopia. The three eyes of three patients that previously underwent scleral buckle surgery were excluded. No other patients had prior intraocular surgeries aside from uncomplicated cataract surgeries. All patients had a best-corrected visual acuity of 20/40 or greater in at least one eye.

The goal of this study was to investigate the influence of the stress exerted by extraocular muscles on the global eye shape and the vitreous chamber of the eye in different directions of gaze by employing distance targets while patients were in the supine position. First, the change in global eye shape was determined by calculating a Dice coefficient,[24] which was used to assess the degree of overlap of the sclera at each eccentric gaze as with that found in primary gaze. Second, changes in VCAV were measured by MRI following shifts in gaze in four cardinal directions and a fixed-effects regression was performed to relate each gaze to VCAV. Specifically, MRI scans were performed while subjects gazed in five directions (primary, left, right, superiorly and inferiorly). Patients maintained their gaze for 3 min on a distance target (a projected 'X' located in standardised locations (10°–15° eccentricity), viewable via a standard head-coil-based mirror). Patients all started with a primary gaze scan and then proceeded in a continuous fashion to the other four gazes in a randomised order. Patients were scanned on a Phillips 3T Achieva scanner with an 8-channel phased-array head coil using a fat-suppressed, axial T2-weighted volumetric scanning sequence (1024×1024 matrix, number of slices=50, voxel size=0.215 mm, slice thickness=1.0 mm, TR=4000 ms, TE=475 ms).

MRI processing algorithm. For each eye, aqueous and vitreous margins were identified semi-automatically by the signal intensity using OsiriX software (OsiriX v5.7, www.osirix-viewer.com), and all tissues outside the globe were removed (figure 1). The subsequent processing stream was constructed as a fully automated pipeline in Matlab 2014a (www.mathworks.com). Voxel intensities were normalised using histogram matching to a reference control eye.[25] Once the intensity was normalised, a threshold of 120 was applied to all eyes. This threshold was chosen by the maximising correlation between MRI and IOLMaster axial lengths. Images were then resampled to 0.2 mm isotropic resolution using trilinear interpolation. FSL/FLIRT (FMRIB's Linear Image Registration Tool)[26] was used to coregister all gaze directions to the centre gaze (linear registration, 6 df). These images were then averaged together to improve signal to noise. A two-dimensional plane was fit through the limbus and centre of the lens (figure 2A) and realigned such that the limbal plane was parallel to the XZ plane of the acquisition matrix (figure 2B). All the unregistered gazes were then co-registered to the aligned mean eye (linear registration, 6 df). The visual axis was approximated as the line normal to the limbal plane passing through the centre of a circle that was best-fit to the limbus itself (figure 2C, D).

Determination of global eye shape and change. The Dice similarity coefficient[24] was used as the main metric of spatial overlap (and therefore global eye shape). A Dice coefficient of 0.0 implies 0% overlap, whereas a coefficient of 1.0 implies 100% overlap (ie, no global eye shape change between the two conditions compared). The Dice coefficient was employed to assess the degree of overlap of the sclera at each eccentric gaze with that found in primary gaze.

VCAV measurements (figure 2). To minimise the effect of blink-induced corneal motion artefact and to average over local areas of irregularities in highly myopic eyes with staphyloma, VCAV was used as the main metric. VCAV was defined as the fluid-filled volume bounded by a cylinder of radius 5.5 mm, centred along the visual axis, between the limbal plane and the anterior surface of the retina, which approximately encompassed the macula region of the retina (figure 2D). An additional benefit of using VCAV was to focus on the volume immediately surrounding the visual axis, and not include the regions of the eye wall prone to the direct effect of extraocular recti muscles at their insertions. All length measurements were taken in the axial (high resolution) plane of the MRI scan. Specifically, the length was taken for all points in the limbal plane within 5.5 mm of the visual axis and summed to generate the final VCAV measure for each eye.

VCAV at each eccentric gaze was compared to the VCAV in primary gaze using a fixed effects regression allowing for subject-specific and eye-specific effects. A linear regression was run relating each gaze (nasal, temporal, upgaze and downgaze, with the reference category of primary gaze) to VCAV, controlling for a full set of subject and eye fixed effects. The inclusion of the fixed effects for every subject and eye (laterality) combination allowed each subject to have a different baseline VCAV for each eye, such that the estimated coefficients for each gaze indicated the within-subject difference in measured VCAV in each eccentric gaze relative to primary gaze. To account for the fact that repeated measurements of eye length were conducted for each subject, we adjusted the SEs to account for clustering at the subject-gaze level. Analysis was performed using Stata 15 software (StataCorp, College Station, TX, USA). Significance was accepted at $p \leq 0.05$.

RESULTS

Subjects exhibited a range of self-reported ethnic backgrounds, including Caucasian (n=29), East Asian (n=9) and African American (n=5). Axial lengths in primary gaze ranged from 27.0 mm to 39.3 mm on IOLMaster, and vitreous chamber axial lengths ranged from 20.4 mm to 32.7 mm on MRI.

The Dice coefficient showed significant gaze-induced eye shape changes in all eccentric gazes as compared with that of the primary gaze ($p<0.0001$, one-sample t-test), but no individual eccentric gaze induced an eye shape change significantly different than that induced by the other eccentric gazes ($p=0.987$) (figure 3). To investigate this phenomenon more closely, we decided to assess for change in the vitreous chamber axial length (defined in figure 2 as the distance along the central, visual axis extending from the lens plane to the sclera). In terms of vitreous chamber axial length comparing the four eccentric gazes to primary gaze, downgaze alone showed a tendency for an increase in vitreous chamber axial length (ie, most points are above the 45° line, figure 4).

VCAV changes were then analysed in order to (1) focus more on axial changes versus eye shape changes near the extraocular muscle insertions and (2) average over local areas of irregularities in highly myopic eyes with staphyloma. A fixed-effects regression compared

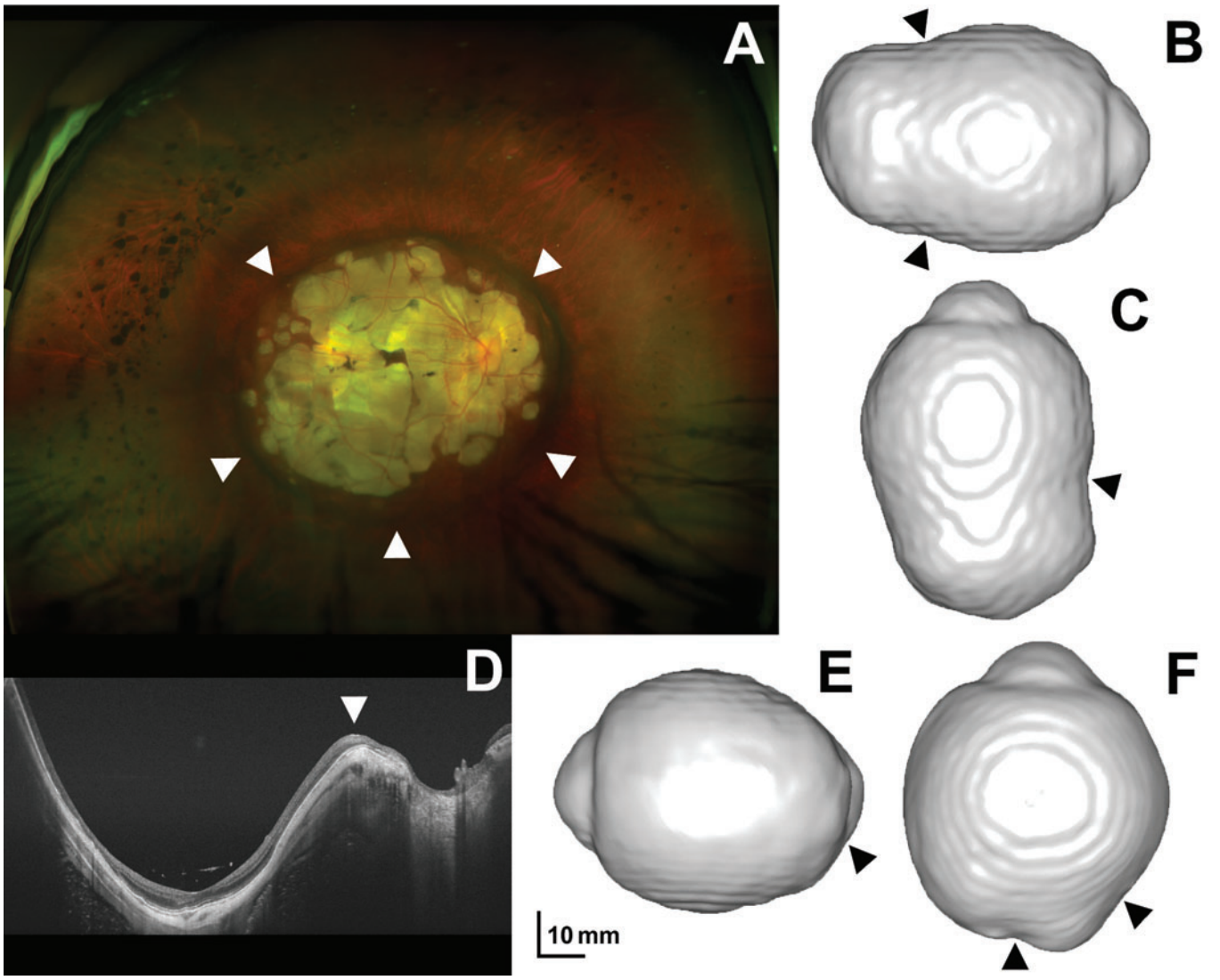

Figure 1 Fundus photography, swept-source optical coherence tomography (SS-OCT) and three-dimensional MRI of patients with posterior staphyloma included in the study. Optos fundus photograph (A) and MRI surface renderings (B—temporal view, C—inferior view) of a right eye with an axial length of 35.4 mm demonstrated a wide macular staphyloma. SS-OCT (D) and MRI surface renderings (E—nasal view, F—superior view) of a right eye with an axial length of 33.8 mm demonstrated a narrow macular staphyloma. The ridges of the staphyloma (A, B, C and right arrow in F) or conus ridge (D, E and left arrow in F) were defined by abrupt changes in scleral curvature (arrowheads). Image adapted with permission from Hoang *et al*.[23]

the relative VCAV at each eccentric gaze versus primary gaze within each subject and eye (right or left) combination (figure 5). In examining VCAV of 82 eyes in the cardinal gazes, accounting for clustered data on the individual patient-gaze level, we found that the mean change in VCAV was statistically insignificant when comparing the primary gaze to the nasal (p=0.272), temporal (p=0.529) or upgaze (p=0.178). However, VCAV increased by +4.79 mm^3 when changing from primary to inferior gaze (p=0.002, 95% CI 1.713 to 7.862) (figure 5).

DISCUSSION

This study demonstrates that while any deviation from primary gaze causes a global shape change in staphylomatous highly myopic eyes, only downgaze induces a reversible, instantaneous elongation in VCAV. Given the association of myopia with excessive near work,[14–17] most prior studies have focused on axial length changes with accommodation or convergence.[18 19] Ghosh and colleagues assessed axial length changes with downgaze using a non-contact optical biometer on a custom-built tilt-adjustable table to measure downward gaze with accommodation in patients with emmetropia and myopia up to −4.06 D[27] and downgaze with far accommodation in patients with emmetropia, low myopia and high myopia (−3.00 D to −6.00 D).[20] They reported an interaction between downward gaze and accommodation on eye axial length, showing an increase of ~8 μm after 10 min in downward gaze with far accommodation (2.5 D), and an additive effect of accommodation (2.5 D) and downgaze (with elongation of ~23 μm after 10 min).[27] They hypothesised that mechanical force from extraocular muscles and/or gravitational effects on the globe may cause a greater level of axial elongation in downward gaze.[27] Ghosh *et al*[20] also reported a greater tendency for axial elongation in the inferonasal gaze (over a 5 min task) with higher refractive error. The present study further supports the biomechanical changes of the globe on downgaze, given that we find VCAV increases with downgaze, while focused on a distant target. Additionally, the present study was performed using MRI in

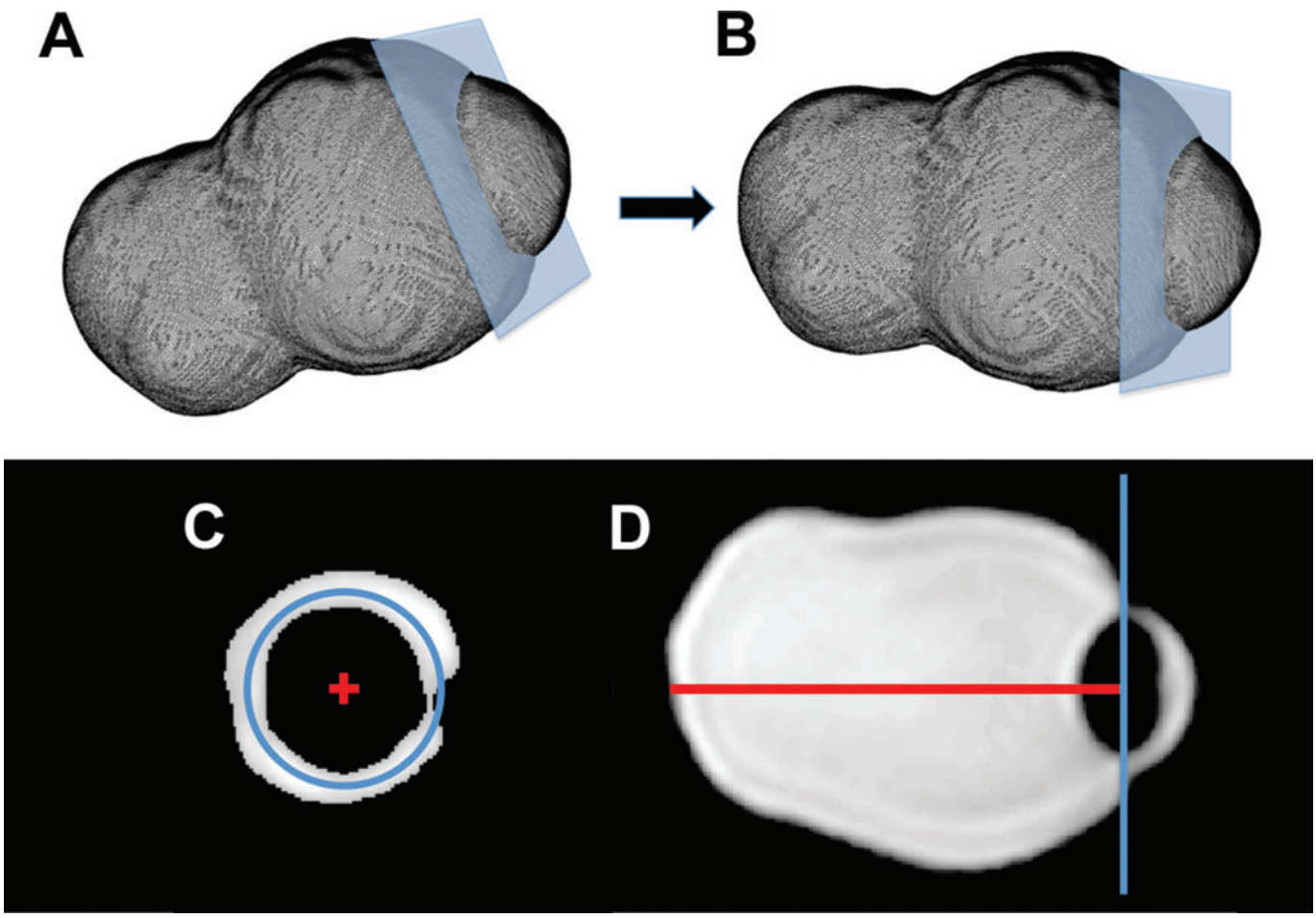

Figure 2 Vitreous chamber axial length measurements of five gazes were performed by a fully automated processing pipeline. All gazes were co-registered to centre gaze by fitting a two-dimensional limbal plane (blue) through the centre of the lens (A) and reorienting the eye until it was parallel to the XZ plane (B). The centre of the limbus (red crosshair) was estimated by fitting a circle through the corneal-scleral boundary (C). Vitreous chamber axial lengths were computed by measuring the distance from the centre of the limbal plane to the anterior surface of the retina along the posterior projection (D; red line). This was repeated for all points in the limbal plane within 5.5 mm of the visual axis and the lengths were summed to generate the final vitreous chamber axial volume for each eye.

the supine position, which reduces any effect gravity may have when using a biometer on an upright subject.

MRI and VCAV Measurements. Because highly myopic eyes with staphyloma are not uniformly spherical, an MRI processing algorithm that locates the visual axis (defined as the line normal to the coronal plane defined by the limbus, that is, the cornea–sclera interface, and intersecting that plane at the centre of a circle best-fit to the limbus) is necessarily more accurate than measurements on multiplanar images. Specifically, unregistered slices derived from multiplanar imaging can result in a high likelihood of error in axial length measurements as the longest dimension may not be parallel to the scanning plane. Moreover, because staphylomatous globes can be locally very irregular and aspherical, we chose to include a cylinder of volume (VCAV, figure 2), approximately bounded by a circle outlining the macula posteriorly and the cornea anteriorly in order to average over small local irregularities. It is important to note that, similar to past studies using MRI measurements of globes,[21] our study employed anisotropic imaging, which has its limitations. There are techniques that achieve higher spatial resolution and more isotropic images, but the selected sequence (using the same parameters as Moriyama *et al*,[21] but with higher field strength to improve signal to noise) was a compromise between the highest resolution obtainable within the amount of time a typical high myopia patient with staphyloma could maintain gaze (limited by the blink reflex, dryness and other environmental factors) and avoid significant motion artefact. Our MRI processing algorithm was customised to provide metrics that could assess gaze-induced global eye shape and VCAV changes, which we feel serve as indicators of scleral biomechanical weakness.

Scleral Remodelling during Myopia Progression May be a Response to Mechanical Stress. Given the structural differences between myopic and emmetropic sclera, a normal force applied on the myopic sclera may cause a greater stretch in comparison with emmetropic eyes. Supporting this notion, animal studies have found that, when compared to emmetropic eyes, myopic eyes have greater scleral creep extensions (in response to sustained strain) and are more vulnerable to the stretching influence of mechanical stress.[28–30] These changes might be present even before the onset of scleral thinning and staphyloma formation in pathologic myopia.[9 11] Taken together with these reports, our findings further support the notion that mechanical stress may result in instantaneous eye shape change, and the magnitude of this change may increase with greater baseline axial length. Extraocular muscle forces, ciliary muscle tone, choroidal muscle tone and intraocular pressure are mechanical factors that may

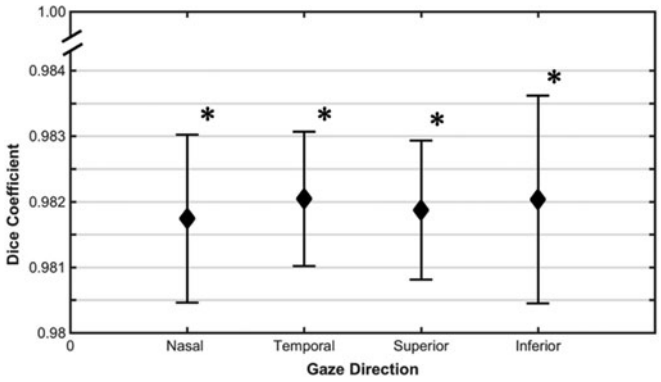

Figure 3 Dice coefficient depiction of the level of scleral overlap in each directional gaze as compared to primary gaze. The Dice coefficient was used as the main metric of spatial overlap (and therefore global eye shape). A Dice coefficient of 0.0 implies 0% overlap whereas a coefficient of 1.0 implies 100% overlap (ie, no global eye shape change between the two conditions compared). A significant globe deformation was found in all eccentric gazes as compared with that of primary gaze. *p<0.001 on a one-sample t-test (compared to 1.0).

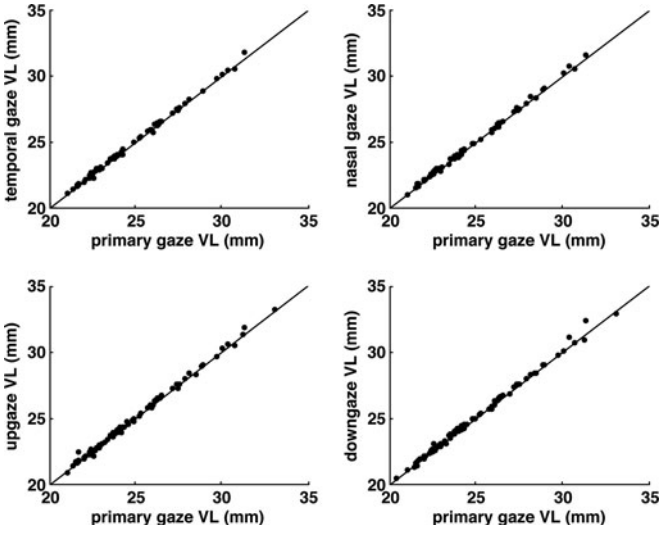

Figure 4 Vitreous chamber length as a function of primary gaze. The diagonal line represents no change in vitreous chamber length. Downgaze showed a tendency for increase in length (ie, most points are above the 45° line). Lengths for nasal, temporal and upgaze were not significantly different from primary gaze. VL, vitreous chamber length.

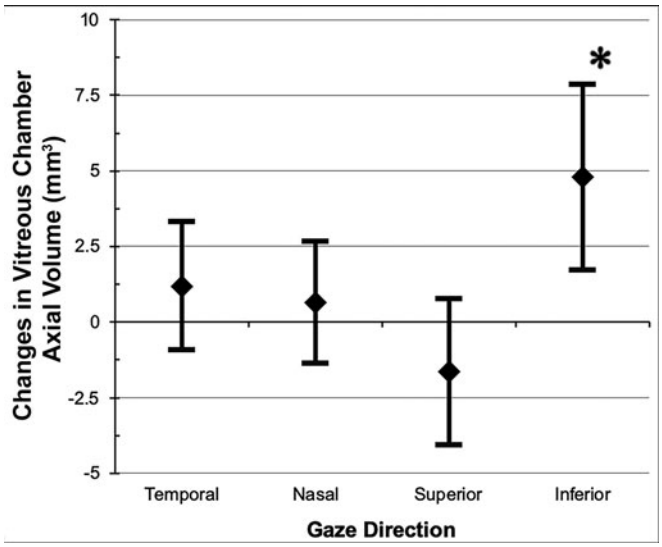

Figure 5 Gaze-induced vitreous chamber axial volume (VCAV) changes in each directional gaze (n=55–82), as compared to the primary gaze. Mean change in VCAV was significantly larger than centre gaze for downward (inferior) gaze direction (p=0.026). Error bars represent 95% CIs. *p<0.05.

alter the structural and biomechanical properties of the sclera. In the present study, significant global eye shape changes in all eccentric gazes were observed, but significant eye elongation was only noted in downgaze, supporting the notion that extraocular muscles exert a non-uniform and asymmetric stress pattern that may be a major mechanical factor acting on the sclera during myopia development. In contrast, ciliary muscle tone, choroidal muscle tone and intraocular pressure are less likely to exert localised stress.

In addition to the optical factors that may drive myopia development, there is evidence suggesting that mechanical stress on the globe, and specifically repeated stress (eg, stress exerted by extraocular muscles during near work), may also play an important role. Grytz *et al*[31] postulated that adaptation of scleral tissue in response to mechanical stress could result in the scleral remodelling mechanism underlying myopia development. Our findings of a significant VCAV elongation in downgaze, likely due to the mechanical influence of extraocular muscles, combined with the results of Ghosh *et al*,[20 27] support the notion that repeated short periods of downgaze (eg, during frequent near work) could have a cumulative, long-term effect of more permanent eye elongation and myopia development, perhaps through a mechanical stress-induced mechanism.

Extraocular Muscles and the Posterior Pole. The posterior pole, in particular, is at greatest risk of pathology arising from the mechanical stress of extraocular muscles. Scleral stiffness of the posterior pole is approximately 60% of that of the anterior pole.[32] Due to their attachment locations at the posterior globe, oblique muscles may produce significant localised stress and contribute to axial elongation.[19] Moreover, pathologic changes in myopia (eg, staphyloma formation, optic disc crescents, choroidal neovascularisation, foveoschisis, macular holes and lacquer cracks) have a propensity to occur in the posterior pole.[33] The combination of localised mechanical stress from the oblique muscles with the fact that the posterior pole is structurally less stiff than elsewhere in the eye may partially explain this propensity. The effect on axial length of upgaze may differ from downgaze due to the fact that the attachments for the superior oblique and inferior oblique muscles are not symmetric, allowing for differing mechanics and resultant local forces, which could lead to differing effects on axial length. On downgaze, both the superior oblique and the inferior rectus would be employed, whereas on upgaze, inferior oblique and superior rectus would be employed. The vector forces exerted by extraocular muscles when moving from primary gaze to downgaze or upgaze are therefore complex, especially since these vector forces are not simply determined by the insertion of the extraocular muscles but also extraocular muscle pulleys.[34]

Summary. The present study is unique in that it focuses on subjects with axial lengths >27 mm and assesses VCAV while subjects are in the supine position, diminishing the effect of gravity in downgaze. Additionally, this study employed a novel processing pipeline to arrive at fully automated length measurements, which reduces subjective bias. Our results, combined with

those from Ghosh *et al*,[20 27] support the notion that short-term stress in the sclera from the extraocular muscles is associated with longer-term scleral remodelling and eye growth. Additionally, since this work suggests it is the downgaze component of near work that may be most associated with eye elongation, our findings support the encouragement of near work in primary gaze (such as desktop computer use) over near work in downgaze (smartphone and tablet use).

Contributors Design of the study: QVH, JG. Conduct of the study: QVH, SC, DJGY, LAY, KBF, JG. Collection of the data: QVH, SC, LAY, KBF, JG. Management of the data: QVH, DJGY, JG. Analysis of the data and interpretation of the data: QVH, JG. Preparation of the manuscript: QVH, DJGY, JG. Review of the manuscript and approval of the manuscript: QVH, SC, DJGY, LAY, KBF, JG.

Funding This publication was supported in part by Career Development Awards from Research to Prevent Blindness (QVH), K08 Grant (QVH, 1 K08 EY023595, National Eye Institute, NIH) the Louis V. Gerstner Jr Scholars Program (QVH), Clinician Scientist Award (QVH, CSA-INVMay0011, National Medical Research Council, Singapore), philanthropic donation from John Cushman (QVH) and The Macula Foundation, New York, NY (LAY). The funding organisations had no role in the design or conduct of this research.

Competing interests None declared.

Provenance and peer review Not commissioned; externally peer reviewed.

Data availability statement Data are available upon reasonable request.

ORCID iDs
Quan V Hoang http://orcid.org/0000-0002-5486-9292
Daryle Jason Go Yu http://orcid.org/0000-0001-8549-7666

REFERENCES

1 Saw SM, Katz J, Schein OD, *et al.* Epidemiology of myopia. *Epidemiol Rev* 1996;18:175–87.
2 Saw SM, Matsumura S, Hoang QV. Prevention and management of myopia and myopic pathology. *Invest Ophthalmol Vis Sci* 2019;60:488–99.
3 Rose K, Smith W, Morgan I, *et al.* The increasing prevalence of myopia: implications for Australia. *Clin Exp Ophthalmol* 2001;29:116–20.
4 Lin LL, Shih YF, Hsiao CK, *et al.* Epidemiologic study of the prevalence and severity of myopia among school children in Taiwan in 2000. *J Formos Med Assoc* 2001;100:684–91.
5 Holden BA, Fricke TR, Wilson DA, *et al.* Global prevalence of myopia and high myopia and temporal trends from 2000 through 2050. *Ophthalmology* 2016;123:1036–42.
6 Dolgin E. The myopia boom. *Nature* 2015;519:276–8.
7 Zadnik K. The Glenn A. Fry award lecture (1995). Myopia development in childhood. *Optom Vis Sci* 1997;74:603–8.
8 Grossniklaus HE, Green WR. Pathologic findings in pathologic myopia. *Retina* 1992;12:127–33.
9 Avetisov ES, Savitskaya NF, Vinetskaya MI, *et al.* A study of biochemical and biomechanical qualities of normal and myopic eye sclera in humans of different age groups. *Metab Pediatr Syst Ophthalmol* 1983;7:183–8.
10 Curtin BJ, Teng CC. Scleral changes in pathological myopia. *Trans Am Acad Ophthalmol Otolaryngol* 1957;62:777–88.
11 Hsiang HW, Ohno-Matsui K, Shimada N, *et al.* Clinical characteristics of posterior staphyloma in eyes with pathologic myopia. *Am J Ophthalmol* 2008;146:102–10.
12 Steidl SM, Pruett RC. Macular complications associated with posterior staphyloma. *Am J Ophthalmol* 1997;123:181–7.
13 Hoang QV, Chen CL, Garcia-Arumi J, *et al.* Radius of curvature changes in spontaneous improvement of foveoschisis in highly myopic eyes. *Br J Ophthalmol* 2016;100:222–6.
14 Saw SM, Chua WH, Hong CY, *et al.* Nearwork in early-onset myopia. *Invest Ophthalmol Vis Sci* 2002;43:332–9.
15 French AN, Morgan IG, Mitchell P, *et al.* Patterns of myopigenic activities with age, gender and ethnicity in Sydney school-children. *Ophthalmic Physiol Opt* 2013;33:318–28.
16 Mutti DO, Mitchell GL, Moeschberger ML, *et al.* Parental myopia, near work, school achievement, and children's refractive error. *Invest Ophthalmol Vis Sci* 2002;43:3633–40.
17 McBrien NA, Adams DW. A longitudinal investigation of adult-onset and adult-progression of myopia in an occupational group. Refractive and biometric findings. *Invest Ophthalmol Vis Sci* 1997;38:321–33.
18 Read SA, Collins MJ, Woodman EC, *et al.* Axial length changes during accommodation in myopes and emmetropes. *Optom Vis Sci* 2010;87:656–62.
19 Greene PR. Mechanical considerations in myopia: relative effects of accommodation, convergence, intraocular pressure, and the extraocular muscles. *Am J Optom Physiol Opt* 1980;57:902–14.
20 Ghosh A, Collins MJ, Read SA, *et al.* Axial length changes with shifts of gaze direction in myopes and emmetropes. *Invest Ophthalmol Vis Sci* 2012;53:6465–71.
21 Moriyama M, Ohno-Matsui K, Hayashi K, *et al.* Topographic analyses of shape of eyes with pathologic myopia by high-resolution three-dimensional magnetic resonance imaging. *Ophthalmology* 2011;118:1626–37.
22 Ang M, Wong CW, Hoang QV, *et al.* Imaging in Myopia: potential biomarkers, current challenges and future developments. *Br J Ophthalmol* 2019;103:855–62.
23 Hoang QV, Chua J, Ang M, *et al.* Imaging in Myopia. Ang M, Wong T, eds. *Updates on Myopia*. Springer, 2020: 219–39.
24 Zou KH, Warfield SK, Bharatha A, *et al.* Statistical validation of image segmentation quality based on a spatial overlap index. *Acad Radiol* 2004;11:178–89.
25 Shapira D, Avidan S, Hel-Or Y. Multiple histogram matching. 2013 IEEE International Conference on Image Processing Proceedings 2013: 2269–73.
26 Jenkinson M, Smith S. A global optimisation method for robust affine registration of brain images. *Med Image Anal* 2001;5:143–56.
27 Ghosh A, Collins MJ, Read SA, *et al.* Axial elongation associated with biomechanical factors during near work. *Optom Vis Sci* 2014;91:322–9.
28 Phillips JR, Khalaj M, McBrien NA. Induced myopia associated with increased scleral creep in chick and tree shrew eyes. *Invest Ophthalmol Vis Sci* 2000;41:2028–34.
29 Curtin BJ. Physiopathologic aspects of scleral stress-strain. *Trans Am Ophthalmol Soc* 1969;67:417–61.
30 Phillips JR, McBrien NA. Form deprivation myopia: elastic properties of sclera. *Ophthalmic Physiol Opt* 1995;15:357–62.
31 Grytz R, Girkin CA, Libertiaux V, *et al.* Perspectives on biomechanical growth and remodeling mechanisms in glaucoma. *Mech Res Commun* 2012;42:92–106.
32 Friberg TR, Lace JW. A comparison of the elastic properties of human choroid and sclera. *Exp Eye Res* 1988;47:429–36.
33 Curtin BJ. The posterior staphyloma of pathologic myopia. *Trans Am Ophthalmol Soc* 1977;75:67–86.
34 Miller JM. Understanding and misunderstanding extraocular muscle pulleys. *J Vis* 2007;7:1–15.